Received: 11 July 2018 | Revised: 12 October 2018 | Accepted: 5 November 2018

DOI: 10.1002/jrs.5524

RESEARCH ARTICLE

WILEY Journal of RAMAN SPECTROSCOPY

The energy of hydrogen bonds in aqueous suspensions of nanodiamonds with different surface functionalization

K.A. Laptinskiy[1,3] | A.N. Bokarev[2] | S.A. Dolenko[3] | I.L. Plastun[2] | O.E. Sarmanova[1] | O.A. Shenderova[4] | T.A. Dolenko[1,5]

[1] Department of Physics, Moscow State University, Moscow, Russia

[2] Department of Applied Information Technology and Communication, Yuri Gagarin State Technical University of Saratov, Saratov, Russia

[3] Skobeltsyn Institute of Nuclear Physics, Lomonosov Moscow State University, Moscow, Russia

[4] Adámas Nanotechnologies, Inc., Raleigh, North Carolina, USA

[5] National Research Nuclear University MEPhI, Moscow, Russia

Correspondence
T.A. Dolenko, Department of Physics, Moscow State University, Moscow, Russia.
Email: tdolenko@mail.ru

Funding information
Russian Science Foundation, Grant/Award Number: 17-12-01481; MEPhI Academic Excellence Project, Grant/Award Number: 02.a03.21.0005 27.08.2013

Abstract

As a result of an experimental study of the Raman scattering valence bands of water in aqueous suspensions of detonation nanodiamonds with different functional surface groups, the energies of hydrogen bonds in suspensions of nanoparticles were calculated for the first time. It is shown that the degree of influence of different functional surface groups of nanodiamonds on hydrogen bonds in aqueous suspension decreases in the series H > polyfunctional surface > OH > COOH. The obtained data are confirmed by modeling of optimized nanodiamond structures in water clusters and theoretical calculations of the bond parameters in these structures by the density functional theory.

KEYWORDS

hydrogen bonds, nanodiamonds aqueous suspension, Raman valence band

1 | INTRODUCTION

Hydrogen bond is a crucial interaction in water, supramolecular, and biological systems. These are hydrogen bonds that partly explain the numerous water anomalies.[1,2] Hydrogen bonds play an important role in organic compounds chemistry, structure of biomacromolecules, polymers, etc.[3] The main problem in the study of hydrogen bonds at present is the almost complete absence of direct methods for determining their energy. For the first time in 2017, Kawai et al.[4] conducted a direct measurement of the strength of the hydrogen bonds between the CO-functionalized tip and the molecules of trinaphtho[3.3.3] propellane and trifluorantheno[3.3.3] propellane with atomic force microscopy. At the same time, there are many indirect methods for estimating the energy of hydrogen bonds in water and other substances.[5–14] Thus, the strength of hydrogen bonds in various substances was determined by theoretical calculations of ab initio molecular simulation studies,[6,7] spectroscopic methods,[8–10] voltammetric methods,[11,12] nuclear magnetic resonance,[13] etc. The obtained values of the energies of hydrogen bonds in water and other systems greatly depend on the method of their determination and therefore differ significantly: According to the estimates of various authors, the energy of hydrogen bonds in water ranges from 8 to 29 kJ/mol.[5] According to the data of the authors[14,15] who applied a theory based on the principles of statistical mechanics for clarification of H-bond thermodynamic properties of water using the experimental temperature and pressure dependences of the water dielectric constant, the enthalpy values of the hydrogen bonds in the water fluctuate

in the range of 6 to 23 kJ/mol. Moreover, to break the hydrogen bond between two water molecules entirely (the separation of oxygen and hydrogen atoms over a considerable distance), the energy of 23.3 kJ/mol is required.[5,14]

Despite its relatively low energy, hydrogen bonds can largely determine the properties of compounds dissolved in water and the dynamics of the system as a whole. There are some papers[16–19] where it was shown that hydrogen bonds significantly influence the properties of nanostructures in water and in solutions of biomacromolecules. This fully concerns nanodiamonds (NDs). As it is known, NDs have wide prospects for their use in nanomedicine as fluorescent markers, adsorbents, and/or drug carriers.[20] However, the effectiveness of the mentioned applications of these carbon nanoparticles relies significantly on understanding the mechanisms of interaction of their surface with the molecules of the environment. Therefore, the study of the interactions of NDs surface groups with water molecules and biomacromolecules is extremely urgent.

In recent decades, many papers devoted to the study of interactions at the ND–water interface have appeared.[21–25] The results of all studies indicate active adsorption of water molecules on the surface of NDs, not only on the hydrophilic regions of the surface of the ND itself,[21–24] but also on its hydrophobic regions,[24] as well as on the hydrophilic regions of sp^2 hybridized carbon, present on the surface of NDs.[25]

The authors[26–34] convincingly showed that detonation NDs (DNDs) dispersed in water and other protic solvents significantly affect the structure of the surrounding layers of solvents, including changing the strength of hydrogen bonds in suspensions. According to the results of the authors,[26] a stable water shell with a thickness of about 0.5 nm is formed in the water around NDs, and the properties of the shell differ significantly from those of bulk water. In their opinion, even trace concentrations of NDs significantly change the physical properties of bulk water, for example, dielectric permittivity.[27] In the paper by Petit et al.,[28] it was found, using X-ray absorption spectroscopy, that the perturbation of the hydrogen bond network caused by ND with sizes of 3–5 nm extends over at least four hydrate layers around the nanoparticle. Moreover, alterations of hydrogen bonds are so great that the electronic structure of water in the ND shell is comparable with the structure of high-density amorphous ice. According to the results of a study of NDs aqueous suspensions,[29–34] dispersed NDs weaken hydrogen bonds in bulk water, and the change of the hydrogen bonds energy mainly depends on the type of surface functional groups of the nanoparticles. With the help of Fourier-transform infrared spectroscopy, Raman spectroscopy, and X-ray absorption spectroscopy of aqueous suspensions of DNDs with different surface functional groups—carboxyl (DND–COOH), hydroxyl (DND–OH), hydrogenated (DND–H), and a polyfunctional surface (DND–poly)—authors[32,33] obtained a series on the degree of influence of DNDs with different functionalization of the surface on the forces of hydrogen bonds in water: DND–H >> DND–OH > DND–poly > DND–COOH > water. As it comes from the obtained series, an abnormally strong attenuation of hydrogen bonds occurs when DND–H is dispersed, and NDs with surface carboxylic groups weaken the hydrogen bonds in suspension less than others. Investigation of the influence of interactions between different surface groups of ND and water molecules on the fluorescent properties of nanoparticles showed that the change in the fluorescence of NDs also depends on the functionalization of their surface. Moreover, a decrease in fluorescence intensity occurs in exact accordance with the above series: the weaker the hydrogen bonds in the suspension, the more intense the fluorescence of NDs.[32,34] A similar dependence of the fluorescent properties on the hydrogen bonding forces was obtained for protic solvents.[30,31] Thus, a significant dependence of the DND fluorescent properties on the hydrogen bonds energy in suspensions was found.

In this paper, for the first time, the energies of hydrogen bonds in aqueous DNDs suspensions with different functional surface groups—carboxyl (DND–COOH), hydroxyl (DND–OH), hydrogenated (DND–H), and a polyfunctional surface (DND–poly)—were calculated. The calculations were carried out using the experimental and theoretical data. For the experimental calculation, the water valence band of Raman spectra of aqueous suspensions of DNDs are used. Theoretical calculations were carried out using the theory of density functional.

2 | METHODS AND MATERIALS

2.1 | Experimental setup

The sizes of DND in aqueous suspensions were measured by the method of dynamic light scattering (DLS) using device ALV-CGS 5000/6010 (Germany).

Zeta potentials of aqueous DND suspensions were measured using Malvern ZetaSizer NanoZS (Malvern, Worcestershire, UK).

Raman spectra of aqueous DND suspensions were registered with a Raman spectrometer. The source of the exciting radiation was an argon laser (λ_{exc} = 488 nm, 300 mW power). The spectra recording system consisted of a monochromator (Acton 2500i, focal length

500 mm, grade 900 grooves/mm) and a charge-coupled device camera (Horiba Jobin Yvon, Syncerity 1024*128 BIUV, the width of entrance slit 25 μm). The practical resolution was 2 cm^{-1}. The temperature of the sample varied from 20°C to 80°C and was controlled and maintained constant during the detection of the spectrum with an accuracy of 0.1°C using a heating element based on the Peltier element. The special construction of the cuvette provided control of the constant volume of the sample and, as a consequence, a constant concentration of DND in the suspension when the temperature of the sample was changed throughout the indicated range. The spectra were normalized to the power of laser radiation, the spectrum accumulation time, detector sensitivity, and the integral intensity of the stretching band.

2.2 | Objects of research

Aqueous suspensions of DNDs with different surface functionalization—DND–H, DND–OH, DND–COOH, and DND–poly—were the objects of the study. The processing and functionalization of the surface of all DNDs are described in detail in Petit et al (2017).[33] Deionized double-distilled water was used to prepare aqueous suspensions. The size of the DND aggregates in water was measured by the DLS, and the zeta potentials of all suspensions were measured on the zeta-sizer. Table 1 shows the main characteristics of the prepared aqueous suspensions.

2.3 | Calculation of the energy of hydrogen bonds in DND suspensions from experimental Raman spectra of water

To quantify the energy of hydrogen bonds in aqueous DND suspensions, the van't Hoff equation (Equation 1), allowing to estimate the effect of temperature on the rate of chemical reaction, was used.

$$\ln(\mathrm{K}) = -\frac{\Delta H}{RT} + \frac{\Delta S}{\mathrm{R}}, \quad (1)$$

where K is the equilibrium constant, ΔH is the enthalpy change, ΔS is the entropy change, and R is the universal gas constant.

The chemical reaction in our case is the conversion of OH groups of water molecules with a strong hydrogen bond into OH groups of water with a weak hydrogen bond under the influence of temperature (with its increase). As is known, Raman scattering valence band of water is sensitive precisely to such changes in the strength of hydrogen bonds.[35–37] Many studies have shown that with increasing water temperature, the intensity of the high-wavenumber region of the valence band caused by vibrations of the OH groups with a weak hydrogen bond increases and the intensity of the low-wavenumber region caused by vibrations of strongly bound OH groups decreases, and the entire band shifts to high wavenumber and narrows.[35–37] Considering this fact, it is necessary to identify two components of the reaction to apply the van't Hoff equation. In our case, these are contributions of OH groups with strong and weak hydrogen bonds into the valence vibration band. These contributions were determined as a result of the decomposition of valence bands of OH groups of DND suspensions into Gaussian components. Obviously, this inverse problem is posed incorrectly for such a wide band. First of all, the number of components, depending on the model chosen, is unknown, and there is a huge variety of models.[5] Genetic algorithms (GAs) were used to decompose the resulting spectral bands into components,[38,39] which made it possible to solve this incorrectly posed inverse problem much more accurately. Namely, the chosen optimization algorithm is less inclined to to fall into local minima of the fitness function, which reduces the probability of ambiguity in the solution and excludes voluntarism in the choice of the water structure model.

TABLE 1 The main characteristics of nanodiamonds in aqueous suspensions

Sample	Size, nm	Zeta-potential, mV	Concentration, mg/ml	pH
DND–H	177.4	+29	0.2	6.97
DND–OH	47.6	+31	1	7.05
DND–COOH	4.6	−42.8	1	6.87
DND–poly	11.5	−37.7	1	5.01

Note. DND: detonation nanodiamond.

2.4 | Decomposition of the bands into components with GAs

The optimization approach used here to decompose a band into components of predefined shape may be described as follows. First, we assume that the possible interaction among the components does not lead to change of their shape—only their parameters can be changed. The studied band is assumed to be a simple sum of the components. Next, we should set the possible shape of a component and its parameters that may change. In

our case, physical considerations prescribe the components to be Gaussian-shaped, with three parameters: amplitude, position of the maximum, and halfwidth. (We could also consider other physically based shapes —e.g., Voigt, but this would additionally increase the number of parameters and reduce the quality of the solution.) Also, we should choose the maximum allowable number of the components—some of them can be then switched off by the optimization algorithm by setting their amplitude to zero; in our case, according to literature data, we should not expect more than five components.

Thus, the shape of the full band can be described by a combination of components having in total $5 \times 3 = 15$ parameters. The fitness function—used to estimate the quality of the solution—is the squared error between the combination of components and the real observed shape of the band.

In a 15-dimensional search space, enumeration-based optimization methods would take an unacceptably large time, and local gradient-based methods are subject to finding some local minimum of the fitness function instead of the global one. Therefore, in this study, we used another class of optimization algorithms—GAs.[39] In our case, GA finds an optimal decomposition of the studied band into Gaussian-shaped components with minimum error (see Figure S1).

2.5 | Calculation of the energy of hydrogen bonds in DND suspensions using the theory of density functional

Molecular modeling was performed by numerical simulation based on the density functional theory,[40] in particular, on the B3LYP functional method.[41] For numerical simulations, we use a split-valence basis set 6-31G(d). For numerical modeling of intermolecular forces in molecular compound, we used the Gaussian 09 program complex,[42] which is traditionally applied for investigations in various areas of computational physics and chemistry and approved by the authors[43,44] and in other investigations.

For accounting of an anharmonicity in intermolecular interaction, we used the following scaling factors for resulted vibrational modes: 0.8742 (range 0–1,000 cm^{-1}); 0.9306 (range 1,000–2,000 cm^{-1}); and 0.956 (range above 2,000 cm^{-1}).

In process of molecular modeling, we used a model based on the simplest diamondoid, adamantane.

Adamantane ($C_{10}H_{16}$) is the basic "building" block for bigger diamond-like structures.[45] In the present work, we consider the modified adamantane, named 1,3,5,7-adamantantetracarboxylic acid (AdTCA; $C_{14}H_{16}O_8$), which contains four carboxylic (—COOH) groups,[46] as an object that approximates a large-size carboxylated ND. The chemical structures of adamantane, AdTCA, and 1-nm-diameter ND with four carboxylic groups are presented on Figure S2.

We compare the calculated infrared (IR) spectra of 1-nm-diameter ND enriched by four —COOH groups and AdTCA with experimental IR spectrum of carboxylated ND for possibility of using AdTCA as an object that approximates a large-size carboxylated ND (Figure 1). The calculated IR spectrum of AdTCA (Figure 1, [4]) is in a good agreement with the calculated IR spectrum of 1-nm-diameter ND enriched by four carboxylic groups (Figure 1, [3]) and the experimental IR spectrum of carboxylated ND (Figure 1, [2]). Thus, the high level of consistency of the characteristic regions in considered spectra and a smaller amount of the required computational time allows to use AdTCA as an object that approximates a large-size carboxylated ND at the level of qualitative estimates of the formation of compounds during molecular modeling. It is also observed that there a lot of C—H groups on the surface of the DND–H (Figure 1, [1]).

3 | RESULTS

3.1 | Raman spectroscopy of DNDs suspensions

The temperature dependences of the Raman spectra of water and aqueous suspensions of DND–H, DND–OH, DND–COOH, and DND–poly were obtained in the

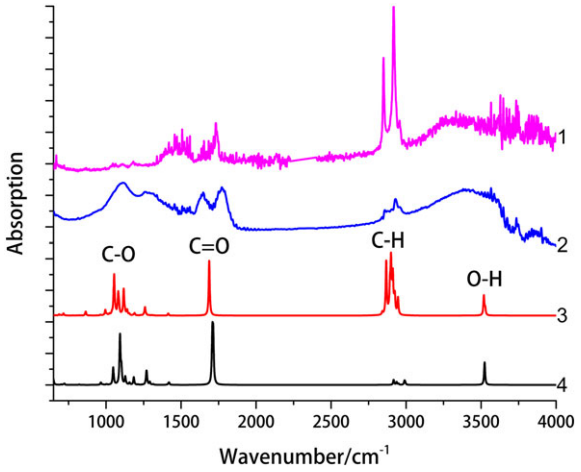

FIGURE 1 Experimental infrared (IR) spectrum of hydrogenated nanodiamond (1) and carboxylated nanodiamond (2) and calculated IR spectra of 1-nm-diameter nanodiamond (3) and 1,3,5,7-adamantanetetracarboxylic acid (4) [Colour figure can be viewed at wileyonlinelibrary.com]

temperature range of 20°C to 80°C in steps of 10°C. As an example, the temperature dependence of the valence band of the OH groups of the DND–COOH aqueous suspension is shown in Figure 2 (In Figures S3–S5, there are temperature dependences of the valence bands of the OH groups of aqueous suspensions DND–H, DND–OH, and DND–poly). The upper part of the valence bands of the OH groups of the above aqueous suspensions at a temperature of 20°C is shown in Figure 3. As can be seen from the obtained data (Figure 2), when the temperature of the samples increases, the intensity of the high-wavenumber region of the water valence band increases, and the intensity of the low-wavenumber region decreases. At a wavenumber of 3,358 cm^{-1}, there is an isosbestic point, the intensity in which does not change with a temperature change.[35,47] According to some models of the water structure, the isosbestic point is the result of an equilibrium between strongly and weakly bound hydrogen bonds of OH groups.[35,47,48] It can be seen from Figure 3 that the ratio of the intensities of the high-wavenumber and low-wavenumber regions of valence bands, that is, the ratio of OH groups with weak and strong hydrogen bonds,[30–33] depends on the type of functional surface groups of DND.

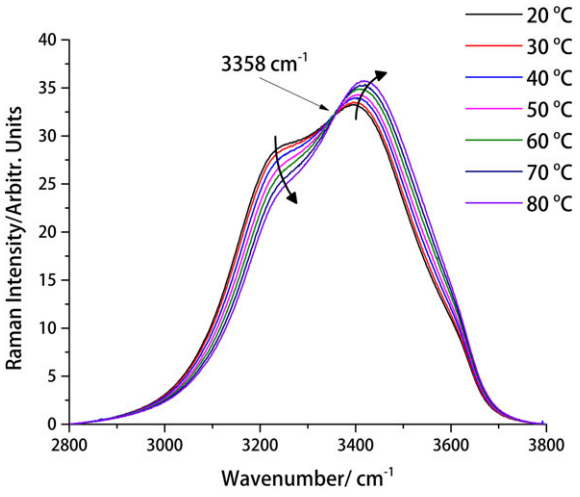

FIGURE 2 The temperature dependence of the valence band of the OH groups of the aqueous suspension of DND–COOH [Colour figure can be viewed at wileyonlinelibrary.com]

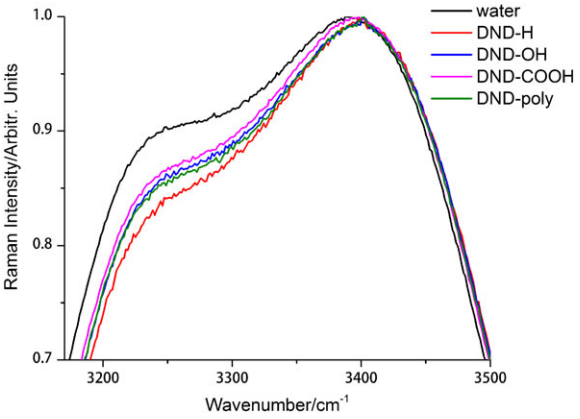

FIGURE 3 The valence bands of OH groups of aqueous suspensions of DND with different surface functionalization at temperature of 20°C. The bands are normalized to a maximum [Colour figure can be viewed at wileyonlinelibrary.com]

The experimental bands of valence vibrations of OH groups of DNDs aqueous suspensions with various surface functionalization obtained at different temperatures were decomposed into Gaussian components. The optimal number of components and the parameters of each component were determined using GA. The use of GA showed that the optimum number of Gaussian components was five (Figure S1). The parameters of these components varied in the following ranges: the maximum position was from 2,500 cm^{-1} to 3,800 cm^{-1}, the area was from 0 to 100,000 arbitrary units, and half-width was from 0 cm^{-1} to 300 cm^{-1}. An example of the obtained decomposition into five components and the errors of this decomposition are presented in Figure 4, and the parameters of the components in Table S1.

Further, for the application of Equation (1), components corresponding to vibrations of OH groups with strong and weak hydrogen bonds were selected, and the dependence of the natural logarithm of the ratio of their total areas—the equilibrium constant of the reaction K—on the inverse temperature was constructed. The "belonging" of the component to OH groups with strong or with weak hydrogen bond was determined in the result of the analysis of the change in the area of the component with a change in temperature (Figure S6): If the component area decreases with increasing temperature, then it corresponds to strongly bound OH groups, and vice versa. As can be seen from Figure S6, under the decomposition of the valence bands of water OH groups

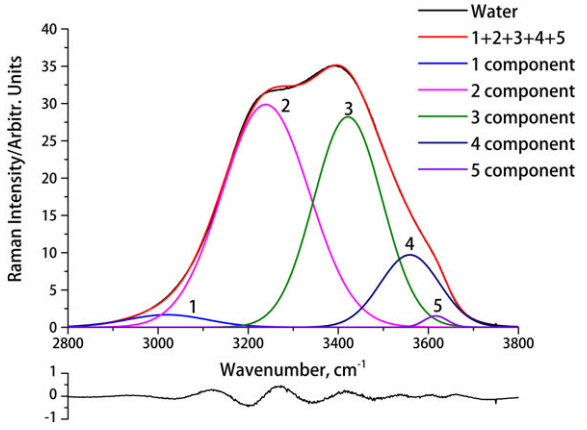

FIGURE 4 Decomposition of valence bands of OH groups into five Gaussian components using general algorithm at temperature of 20°C. The lower part of the figure shows the approximation errors [Colour figure can be viewed at wileyonlinelibrary.com]

into five components with the help of GA, one can distinguish two components whose contribution to the band of valence OH groups decreases (with maxima in the region of 3,015 cm^{-1} and 3,235 cm^{-1}) and three components whose contribution increases (with maxima in the region of 3,420 cm^{-1}, 3,560 cm^{-1}, 3,617 cm^{-1}). It should be noted that the isosbestic point of the temperature dependence of valence bands of OH groups of the samples actually divides all the components into two groups—those whose contribution to the total intensity of the bands decreases with increasing temperature and those whose contribution increases (Figure S6).

Figure 5 shows the calculated dependences of the natural logarithm of the equilibrium constant K on the inverse temperature for water. Similar dependences were obtained for aqueous DND suspensions. All the lnK(1/*T*) dependences are well approximated by a linear function.

Equation (1) was used to calculate the enthalpy change ΔH during conversion of the OH groups with strong hydrogen bonds into OH groups with weak hydrogen bonds in water and in aqueous DND suspensions with different surface functionalization. One should note that the intensity of the valence vibration band of water is proportional to the number of OH groups, and, according to various models of water structure and quantitative estimates, the average number of hydrogen bonds per one molecule of water varies[49] from two to four. Thus, on the average, there are 1.5 hydrogen bonds per one OH group in the water. According to this fact, the values of enthalpy change in hydrogen bonds in water and aqueous suspensions of DNDs with different surface functionalization with increasing temperature were calculated. The results are shown in Table 2.

As can be seen from Table 2, all the investigated DND samples weaken the forces of hydrogen bonds in aqueous suspensions to varying degrees. The greatest weakening of hydrogen bonds was observed when DNDs with a hydrogenated surface are added, the least attenuation was found for carboxylated DNDs. Taking into account the calculated values of the enthalpy change, a series was determined according to the degree of influence of various functional surface groups of the DND on the hydrogen bonds in the aqueous suspension:

$$\text{DND}\text{–}H > \text{DND}\text{–}poly > \text{DND}\text{–}OH > \text{DND}\text{–}COOH \quad (2)$$

Similar results were qualitatively obtained by the authors of the article earlier from the change in the shape of the Raman scattering valence bands of water and X-ray absorption spectroscopy of the studied suspensions.[32,33] It is interesting to note that in the case of the selected concentrations of the studied DND in water, the total surface areas of the DND–poly, DND–COOH, and DND–OH differ from each other within the margin of the order (Table 1), and the total surface area of the DND–H particles is two to three orders less than the surface area of any of the studied nanoparticles. However, the influence of the DND–H particles is significantly greater compared with all other nanoparticles. This suggests an abnormally strong influence of the DND–H surface groups on hydrogen bonds in the aqueous environment.[33] In addition, the total surface area of the DND–COOH is the largest compared with that of all other nanoparticles, and these NDs have the least influence on the hydrogen bonds. One could take this reasoning as a contradiction if all the functional groups were the same. However, our earlier results[32,33] and the content in this article allow us to conclude about the distinct properties of each of the functional groups under study with respect to their influence on hydrogen bonds in the aqueous environment. The quantitative estimates of the energy of hydrogen

TABLE 2 Values of the enthalpy change of hydrogen bonds in water and aqueous suspensions of detonation nanodiamonds (DNDs) with different functionalization with increasing temperature

	Genetic algorithm five components	Theoretical calculations
Sample	**$-\Delta H$, kJ/mol**	**$-\Delta H$, kJ/mol**
Water	15.5 ± 0.2	14.2
DND–COOH	14.0 ± 0.2	13.0
DND–OH	13.5 ± 0.1	12.8
DND–poly	13.1 ± 0.1	
DND–H	12.7 ± 0.1	12.6

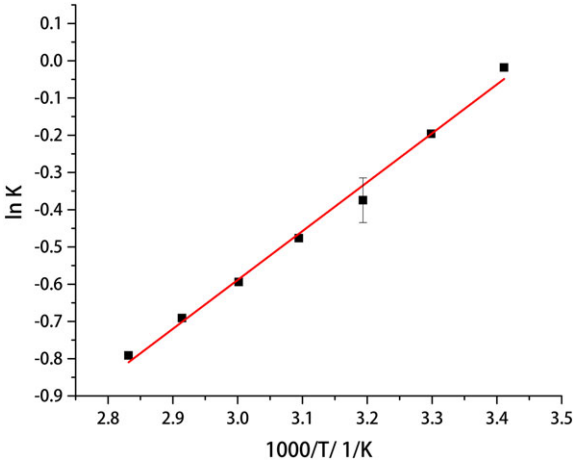

FIGURE 5 Dependence of the natural logarithm of the equilibrium constant on the inverse temperature for water [Colour figure can be viewed at wileyonlinelibrary.com]

bonds obtained for the first time and presented in this paper confirmed the obtained series (2).

3.2 | Theoretical calculations of the hydrogen bonds energy in aqueous suspensions of DNDs

Optimized DNDs structures with functional surface groups COOH (Figure 6), OH (Figure S7), and H (Figure S8) in the environment of 100 molecules of the water cluster and the parameters of the bonds in these structures were calculated with the help of the density functional theory.

For all optimized DNDs complexes in the water cluster, wavenumber shifts $\Delta\nu$ of the symmetric valence vibrations of OH groups in the DND suspensions were calculated in comparison with the symmetric valence vibrations of the OH groups directly in the water cluster. The energy of the hydrogen bonds between the functional surface groups of the DND and the surrounding water molecules was calculated by the Iogansen formula[50,51]:

$-\Delta H = 0.3\cdot\sqrt{\Delta\nu} - 40$. Table 2 presents the calculated parameters of hydrogen bonds in optimized configurations.

One should note that the values of the energies of hydrogen bonds in aqueous suspensions of DNDs with different functionalization, presented in Table 2, are obtained for the first time.

According to the results presented in Table 2, the theoretical and experimental values of the hydrogen bonds energy in aqueous suspensions of DNDs with different surface functionalizations are consistent with each other, taking into account what was said in the introduction about the energy spread of hydrogen bonds found by various methods.[5] Nevertheless, the values obtained by us experimentally and theoretically confirm the earlier series (1) regarding the degree of influence of different surface groups of DNDs on the energy of hydrogen bonds with surrounding water molecules. Our results show the weakening of hydrogen bonds in comparison with hydrogen bonds in water by 18% for DND–H, by 15% for DND–poly, by 13% for DND–OH, and by 10% for DND–COOH. As an example of changes in the hydrogen bonds energy as a result of the compounds interaction with water molecules, one can cite the results of theoretical calculations of small model systems containing HOH and H2CO by Levitt and Perutz[52]: compared with the energy of hydrogen bonds in water, HOH···OCH2 hydrogen bonds weaken by 33%, HOCH ···OH2 by 59%, and HOCH···OH2 (cyclic) by 2%.

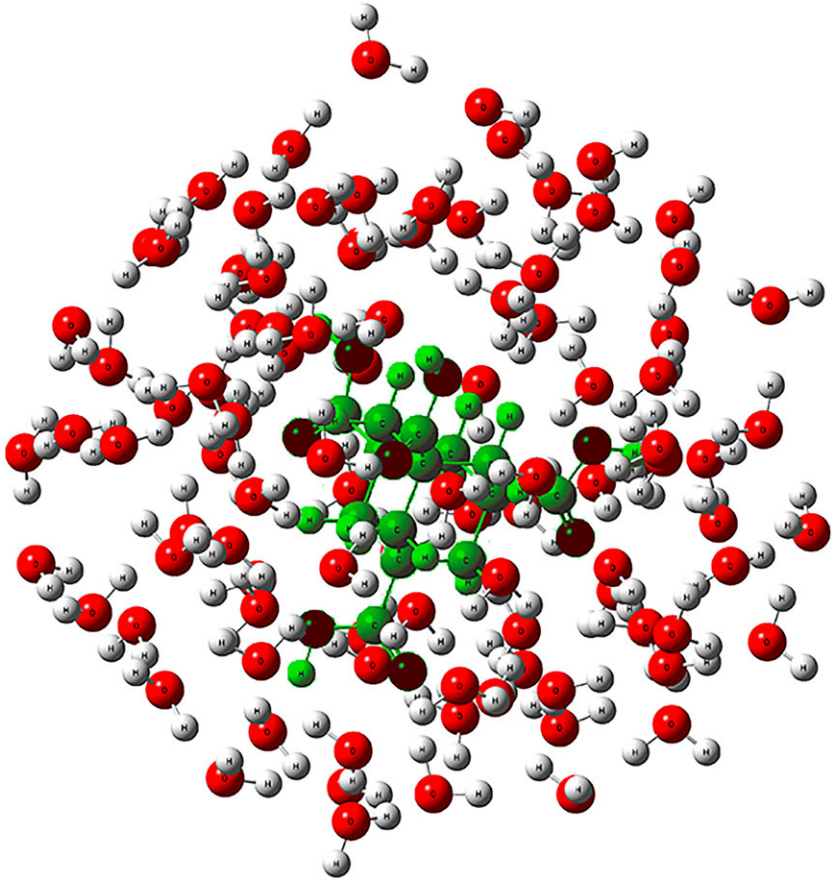

FIGURE 6 Structure of the molecular complex of 1,3,5,7-adamantane tetracarboxylic acid with 100 water molecules [Colour figure can be viewed at wileyonlinelibrary.com]

4 | CONCLUSION

In the article, the numerical values of the hydrogen bonds energy in aqueous suspensions of DNDs with different surface functional groups—COOH, OH, H, and a polyfunctional surface—were obtained for the first time. The values of the energy of hydrogen bonds were obtained in two ways: from the temperature dependences of the experimental Raman spectra of aqueous suspensions of the DNDs with the help of the van't Hoff equation and as a result of modeling and theoretical calculations using the density functional theory. The dependence of the degree of influence of different DNDs on the hydrogen bonds forces in suspensions on the type of the surface functionalization of nanoparticles earlier obtained by the authors of this article, DND–H > DND–poly > DND–OH > DND–COOH, was confirmed numerically. The obtained results once again demonstrated the essential role of the surface chemistry of nanoparticles in studying the processes occurring in their suspensions.

ACKNOWLEDGEMENTS

This study has been performed at the expense of the grant of Russian Science Foundation (project No 17-12-01481; K.A.L. and O.E.S.—planning and conducting of the experiment, calculations, and discussion of results) and was partially supported by the MEPhI Academic Excellence Project contract, No. 02.a03.21.0005, 27.08.2013 (T. A.D.—discussion of results).

ORCID

K.A. Laptinskiy https://orcid.org/0000-0003-2592-5942
S.A. Dolenko https://orcid.org/0000-0001-6214-3195
I.L. Plastun https://orcid.org/0000-0002-1246-8896
T.A. Dolenko https://orcid.org/0000-0003-2884-8241

REFERENCES

[1] H. Tanaka, *Europhys. Lett.* **2000**, *50*(3), 340.

[2] K. Stokely, M. G. Mazza, H. E. Stanley, G. Franzese, *PNAS* **2010**, *107*(4), 1301.

[3] D. Nelson, M. Cox, *Lehninger Principles of Biochemistry*, W.H. Freeman, New York **2012**.

[4] S. Kawai, T. Nishiuchi, T. Kodama, P. Spijker, R. Pawlak, T. Meier, A. S. Foster, *Sci. Adv.* **2017**, *3*(5), e1603258.

[5] M. Chaplin http://www1.lsbu.ac.uk/water/water_structure_science.html (accessed 10 July 2018).

[6] E. Guardia, I. Skarmoutsos, M. Masia, *J.Phys.Chem.B* **2015**, *119*, 8926.

[7] L. Sapir, D. Harries, *J. Chem. Theory Comput.* **2017**, *13*(6), 2851.

[8] J. Yarwood, G. N. Robertson, *Nature* **1975**, *257*(5521), 41.

[9] B. Auer, R. Kumar, J. R. Schmidt, J. L. Skinner, *PNAS* **2007**, *104*(36), 14215.

[10] D. H. Dagade, S. S. Barge, *Chem. Phys. Chem.* **2016**, *17*(6), 902.

[11] M. E. Tessensohn, M. Lee, H. Hirao, R. D. Webster, *Chem. Phys. Chem.* **2015**, *16*(1), 160.

[12] N. Gupta, H. Linschitz, *J. Am. Chem. Soc.* **1997**, *119*(27), 6384.

[13] A. V. Afonin, A. V. Vashchenko, M. V. Sigalov, *Org. Biomol. Chem.* **2016**, *14*, 11199.

[14] F. Hakem, A. Boussaid, H. Benchouk-Taleb, M. R. Bockstaller, *J. Chem. Phys.* **2007**, *127*, 224106.

[15] S. J. Suresh, V. M. Naik, *J. Chem. Phys.* **2000**, *113*, 9727.

[16] O. Byl, J. C. Liu, Y. Wang, W. L. Yim, J. K. Johnson, J. T. Yates, *J. Am. Chem. Soc.* **2006**, *128*, 12090.

[17] D. C. Tien, C. Y. Liao, J. C. Huang, K. H. Tseng, J. K. Lung, T. T. Tsung, W. S. Kao, T. H. Tsai, T. W. Cheng, B. S. Yu, H. M. Lin, L. Stobinski, *Rev. Adv. Mater. Sci.* **2008**, *18*, 750.

[18] Q. Chen, Q. Wang, Y. C. Liu, T. Wu, *J. Chem. Phys.* **2014**, *140*, 214507.

[19] H. Wang, X. Zhao, X. Han, Z. Tang, S. Liu, W. Guo, C. Deng, Q. Guo, H. Wang, F. Wu, X. Meng, J. P. Giesy, *Sci. Total Environ.* **2017**, *586*, 817.

[20] K. Turcheniuk, V. N. Mochalin, *Nanotechnology* **2017**, *28*, 252001.

[21] S. Ji, T. Jiang, K. Xu, S. Li, *Appl. Surf. Sci.* **1998**, *133*(4), 231.

[22] M. V. Korobov, N. A. Avramenko, A. G. Bogachev, N. N. Rozhkova, E. Osawa, *J. Phys. Chem. C* **2007**, *111*(20), 7330.

[23] S. Stehlik, T. Glatzel, V. Pichot, R. Pawlak, E. Meyer, D. Spitzer, B. Rezek, *Diamond Relat. Mater.* **2016**, *63*, 97.

[24] O. Manelli, S. Corni, M. C. Righi, *J. Phys. Chem. C* **2010**, *114*(15), 7045.

[25] E. Z. Pina-Salazar, K. Urita, T. Hayashi, R. Futamura, F. Vallejos-Burgos, J. Włoch, P. Kowalczyk, M. Wisńiewski, T. Sakai, I. Moriguchi, A. P. Terzyk, E. Osawa, K. Kaneko, *Langmuir* **2017**, *33*, 11180.

[26] S. S. Batsanov, E. V. Lesnikov, D. A. Dan'Kin, D. M. Balakhanov, *Appl. Phys. Lett.* **2014**, *104*(13), 133105.

[27] S. S. Batsanov, S. M. Gavrilkin, A. S. Batsanov, K. B. Poyarkov, I. I. Kulakova, D. W. Johnsonb, B. G. Mendis, *J. Mater. Chem.* **2012**, *22*, 11166.

[28] T. Petit, H. Yuzawa, M. Nagasaka, R. Yamanoi, E. Osawa, N. Kosugi, E. F. Aziz, *J. Phys. Chem. Lett.* **2015**, *6*, 2909.

[29] T. Petit, M. Pflüger, D. Tolksdorf, J. Xiao, E. F. Aziz, *Nanoscale* **2015**, *7*, 2987.

[30] T. A. Dolenko, S. A. Burikov, K. A. Laptinskiy, J. M. Rosenholm, O. A. Shenderova, I. I. Vlasov, *Phys. Status Solidi A* **2015**, *212*(11), 2512.

[31] A. M. Vervald, S. A. Burikov, O. A. Shenderova, N. Nunn, D. O. Podkopaev, I. I. Vlasov, T. A. Dolenko, *J. Phys. Chem. C* **2016**, *120*, 19375.

[32] T. A. Dolenko, S. A. Burikov, J. M. Rosenholm, O. A. Shenderova, I. I. Vlasov, *J. Phys. Chem. C* **2012**, *116*(45), 24314.

[33] T. Petit, L. Puskar, T. Dolenko, S. Choudhury, E. Ritter, S. Burikov, K. Laptinskiy, Q. Brustowski, U. Schade, H. Yuzawa, M. Nagasaka, N. Kosugi, M. Kurzyp, A. Venerosy, H. Girard, J. C. Arnault, E. Osawa, N. Nunn, O. Shenderova, E. F. Aziz, *J. Phys. Chem. C* **2017**, *121*, 5185.

[34] P. Reineck, D. W. M. Lau, E. R. Wilson, K. Fox, M. R. Field, C. Deeleepojananan, V. N. Mochalin, B. C. Gibson, *ACS Nano* **2017**, *11*(11), 10924.

[35] G. E. Walrafen, M. R. Fisher, M. S. Hokmabadi, W. H. Yang, *J. Chem. Phys.* **1986**, *85*, 6970.

[36] T. A. Dolenko, I. V. Churina, V. V. Fadeev, S. M. Glushkov, *J. Raman Spectrosc.* **2000**, *31*(8-9), 863.

[37] G. E. Wallrafen, *J. Chem. Phys.* **1968**, *48*(1), 244.

[38] GeneHunter Add-In for Microsoft Excel from Ward Systems Group, Inc. http://www.wardsystems.com/genehunter.asp

[39] D. E. Goldberg, *Genetic Algorithms in Search, Optimization, and Machine Learning*, Addison-Wesley, Boston **1989**.

[40] W. Kohn, *Rev. Mod. Phys.* **1999**, *71*, 1253.

[41] J. Pople, *Angew. Chem.* **1999**, *38*(13-14), 1894.

[42] M. J. Frisch, G. W. Trucks, H. B. Schlegel, G. E. Scuseria, M. A. Robb, J. R. Cheeseman, G. Scalmani, V. Barone, B. Mennucci, G. A. Petersson, H. Nakatsuji, M. Caricato, X. Li, H. P. Hratchian, A. F. Izmaylov, J. Bloino, G. Zheng, J. L. Sonnenberg, M. Hada, M. Ehara, K. Toyota, R. Fukuda, J. Hasegawa, M. Ishida, T. Nakajima, Y. Honda, O. Kitao, H. Nakai, T. Vreven, J. A. Montgomery Jr., J. E. Peralta, F. Ogliaro, M. Bearpark, J. J. Heyd, E. Brothers, K. N. Kudin, V. N. Staroverov, R. Kobayashi, J. Normand, K. Raghavachari, A. Rendell, J. C. Burant, S. S. Iyengar, J. Tomasi, M. Cossi, N. Rega, J. M. Millam, M. Klene, J. E. Knox, J. B. Cross, V. Bakken, C. Adamo, J. Jaramillo, R. Gomperts, R. E. Stratmann, O. Yazyev, A. J. Austin, R. Cammi, C. Pomelli, J. W. Ochterski, R. L. Martin, K. Morokuma, V. G. Zakrzewski, G. A. Voth, P. Salvador, J. J. Dannenberg, S. Dapprich, A. D. Daniels, O. Farkas, J. B. Foresman, J. V. Ortiz, J. Cioslowski, D. J. Fox, *Gaussian 09, Revision A.1*, Gaussian, Inc., Wallingford, CT **2009**.

[43] K. A. Laptinskiy, E. N. Vervald, A. N. Bokarev, S. A. Burikov, M. D. Torelli, O. A. Shenderova, I. L. Plastun, T. A. Dolenko, *J. Phys. Chem. C* **2018**, *122*, 11066.

[44] A. N. Bokarev, I. L. Plastun, *Nanosyst.: Phys., Chem., Math.* **2018**, *9*(3), 370.

[45] R. C. Fort Jr., P. v. R. Schleyers, *Chem. Rev.* **1964**, *64*(3), 277.

[46] O. Ermer, *J. Am. Chem. Soc.* **1988**, *110*(12), 3747.

[47] G. E. Walrafen, M. H. Hokmabadi, W. H. Yang, *J. Chem. Phys.* **1986**, *85*, 6964.

[48] J. D. Worley, I. M. Klotz, *J. Chem. Phys.* **2004**, *45*, 2868.

[49] A. K. A. Rastogi, S. Suresh, Hydrogen Bond Interactions Between Water Molecules in Bulk Liquid, Near Electrode Surfaces and Around Ions. Thermodynamics - Physical Chemistry of Aqueous Systems, InTech, **2011.**

[50] A. V. Iogansen, *Spectrochim. Acta, Part A* **1999**, *55*(7), 1585.

[51] L. M. Babkov, J. Baran, N. A. Davydova, K. E. Uspenskiy, *J. Mol. Struct.* **2006**, *792 − 793*, 68.

[52] M. Levitt, M. F. Perutz, *J.Mol.Biol.* **1988**, *201*, 751.

SUPPORTING INFORMATION

Additional supporting information may be found online in the Supporting Information section at the end of the article.

How to cite this article: Laptinskiy KA, Bokarev AN, Dolenko SA, et al. The energy of hydrogen bonds in aqueous suspensions of nanodiamonds with different surface functionalization. *J Raman Spectrosc*. 2019;50:387–395. https://doi.org/10.1002/jrs.5524